FEBS Letters

An international journal for the rapid publication of short reports in biochemistry, biophysics and molecular cell biology

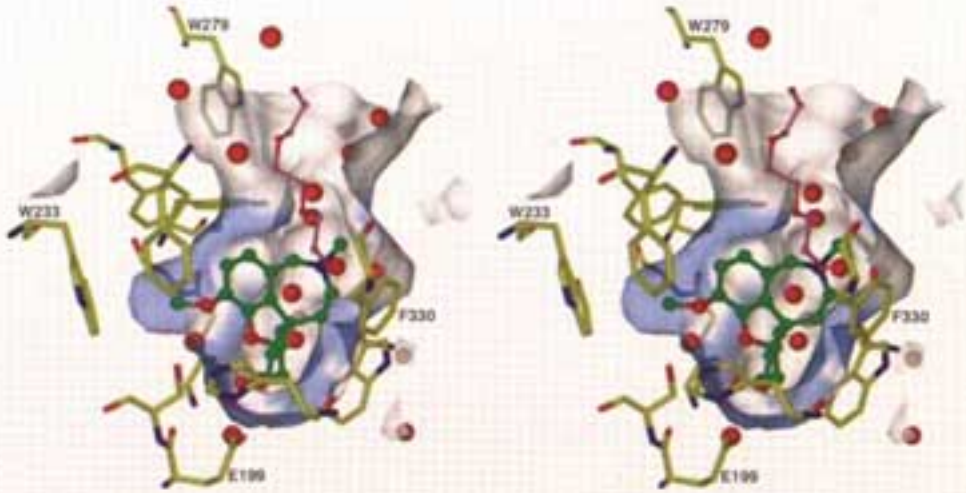

Published by Elsevier
on behalf of the
Federation of European
Biochemical Societies
ISSN 0 014 5793

Last number of this volume
Volume 463
Number 3
17 December 1999

Structure of acetylcholinesterase complexed with (−)-galanthamine at 2.3 Å resolution

H.M. Greenblatt[a], G. Kryger[a], T. Lewis[b], I. Silman[c], J.L. Sussman[a,*]

[a] *Department of Structural Biology, Weizmann Institute of Science, Rehovot 76100, Israel*
[b] *Zeneca Agrochemicals, Jealott's Hill Research Station, Bracknell, Berkshire RG12 6EY, UK*
[c] *Department of Neurobiology, Weizmann Institute of Science, Rehovot 76100, Israel*

Received 8 November 1999

Edited by Shmuel Shaltiel

Abstract (−)-Galanthamine (GAL), an alkaloid from the flower, the common snowdrop (*Galanthus nivalis*), shows anticholinesterase activity. This property has made GAL the target of research as to its effectiveness in the treatment of Alzheimer's disease. We have solved the X-ray crystal structure of GAL bound in the active site of *Torpedo californica* acetylcholinesterase (*Tc*AChE) to 2.3 Å resolution. The inhibitor binds at the base of the active site gorge of *Tc*AChE, interacting with both the choline-binding site (Trp-84) and the acyl-binding pocket (Phe-288, Phe-290). The tertiary amine group of GAL does not interact closely with Trp-84; rather, the double bond of its cyclohexene ring stacks against the indole ring. The tertiary amine appears to make a non-conventional hydrogen bond, via its N-methyl group, to Asp-72, near the top of the gorge. The hydroxyl group of the inhibitor makes a strong hydrogen bond (2.7 Å) with Glu-199. The relatively tight binding of GAL to *Tc*AChE appears to arise from a number of moderate to weak interactions with the protein, coupled to a low entropy cost for binding due to the rigid nature of the inhibitor.

Key words: Cholinesterase; Alzheimer's disease; Natural product; Herbal medicine; Galanthamine

1. Introduction

According to the 'cholinergic hypothesis', Alzheimer's disease (AD) is associated with cholinergic insufficiency [1–3]. This serves as the rationale for use of cholinergic agonists [4,5] and cholinesterase inhibitors [6,7] for the symptomatic treatment of AD in its early stages. Indeed, cholinesterase inhibitors are the only drugs so far approved for treatment of AD. These drugs include natural substances, such as the alkaloids, physostigmine [8] and huperzine A [9], and synthetic compounds, such as tacrine, under its trade name, Cognex® [10], SDZ ENA-713, also known as Exelon® [11], metrifonate [12] and E2020, under its trade name, Aricept® [13,14].

Galanthamine (4a,5,9,10,11,12-hexahydro-3-methoxy-11-methyl-6H-benzofuro[3a,3,2-ef][2]-benzazepin-6-ol; GAL; see Fig. 1) is an alkaloid found in the bulbs and flowers of the common snowdrop (*Galanthus nivalis*) and of several other members of the *Amaryllidaceae* family. The active ingredient was discovered accidentally by a Bulgarian pharmacologist in wild Caucasian snowdrops in the early 1950s [15]. The plant extracts were used initially to treat nerve pain and poliomyelitis. As a natural compound, GAL has since been tested for use in anesthesiology [16] and for treatment of many human ailments, from facial nerve paralysis to schizophrenia and various dementia [17–19]. It is marketed as a hydrobromide salt under the name Reminyl™.

GAL displays 53-fold selectivity for human erythrocyte acetylcholinesterase (AChE) over butyrylcholinesterase (BChE), with IC_{50} values of 0.35 μM for erythrocyte AChE and 18.6 mM for plasma BChE [20]. An IC_{50} of 652 nM has been recorded for *Torpedo californica* AChE (*Tc*AChE) (T. Lewis and C. Personeni, unpublished results). Interestingly, it displays 10-fold lower potency towards human brain AChE than towards the erythrocyte enzyme [21]. In addition to serving as a cholinesterase inhibitor, GAL is also a nicotinic activator, acting both on ganglionic and muscle receptors [22,23] and on nicotinic receptors in the brain [24]. Nicotinic modulation represents a new and promising approach in Alzheimer research [25–30]. A recent report suggests that stimulation of nicotinic receptors may be associated with diminished appearance of amyloid plaques, one of the hallmarks of AD [31]. The double action of GAL, as both an anticholinesterase and a nicotinic activator, has rendered it a promising candidate drug for the treatment of AD. Indeed, phase III clinical trials in Europe for the treatment of AD were recently completed [32], although approval has not yet been granted.

Structure-based drug design is an important tool in the development of second-generation candidate drugs based on a lead compound [28,33–35]. Although computerized docking programs are becoming increasingly sophisticated, the X-ray analysis of a ligand-protein structure often yields crucial information. Indeed, in the case of AChE, determination of the three-dimensional (3D) structures of the appropriate ligand-AChE complexes was a prerequisite for making correct structural assignments for huperzine A [36] and E2020 [14], as well as for the snake venom toxin, fasciculin [37]. In the case of GAL, too, docking protocols suggest more than one possible orientation (Fletcher, R., Viner, R., Lewis, T., unpublished results). Determination of the 3D structure of a GAL-AChE complex would obviously resolve the issue. Furthermore, knowledge of the structure of the complex would also allow us to rationalize results of recent synthetic modifications [38] aimed at improving binding characteristics of GAL to AChE. In the following, we present the X-ray crystal structure, at 2.3 Å resolution, of the GAL-*Tc*AChE complex.

*Corresponding author. Fax: (972)-8-934 4159.
E-mail: joel.sussman@weizmann.ac.il

PII: S0014-5793(99)01637-3

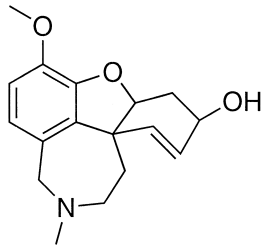

Fig. 1. GAL.

2. Materials and methods

2.1. Crystallization and data collection

*Tc*AChE was purified and crystallized as described [36]. GAL was purchased from Sigma (G1160, lot # 56H0191, hydrobromide form). Three crystals of *Tc*AChE were harvested and transferred to a drop containing mother liquor and 10 mM GAL. After 2 days, they were transferred to a second solution of mother liquor containing 20 mM GAL. All work was done at 4°C. After 2 more days, a crystal was transferred to oil, mounted in a cryo-loop, placed on the goniostat and flash-cooled to 100 K in an Oxford Systems Cryostream. The X-ray source was a Rigaku FR-C rotating anode running at 50 KV/100 mA. Images were collected with a Rigaku RAXIS-IIC. Data collection statistics are summarized in Table 1. Data processing was carried out with DENZO/SCALEPACK [39]. Data were truncated with the CCP4 [40] program TRUNCATE, and a list of randomly generated test reflections was added from a master list for the trigonal crystal form of *Tc*AChE using CAD and FREERFLAG. Reflections were output with MTZ2VARIOUS to a format suitable for CNS.

2.2. Refinement

The protein was refined in CNS [41], initially by use of rigid body refinement. Subsequently, difference maps (Fo−Fc) and 2Fo−Fc maps were used to fit the GAL molecule, two carbohydrate moieties and 93 water molecules (to 4.5σ). The initial electron density for the inhibitor was unambiguous, as seen in Fig. 2. The program XtalView [42] was used for all model building. The model used for GAL was taken from the crystal structure ([43]; CSD code SIBHAM) of the neutral compound. Individual B-refinement was carried out, followed by simulated annealing (torsion dynamics mode [44]), followed again by individual B-factor refinement. Inspection of positive peaks in difference maps to 4σ showed an additional 51 water molecules, as well as a continuous stretch of density near the top of the active site gorge which was modeled as a PEG trimer. Inspection of the entire protein resulted in a few minor changes to side chain positions outside the area of the active site. The model was further refined by positional maximum-likelihood minimization and by individual B-factor refinement. The results are summarized in Table 2.

Table 1
Collection and processing statistics

Oscillation angle	0.5°						
Total number of frames	72						
Total number of reflections	215 846						
Resolution range	30–2.3 Å						
Number of unique reflections	43 422						
Redundancy	0	1	2	3	4	>5	
% Reflection	1.3	20.8	47.1	24.8	5.0	1.0	
Average redundancy (weighted)	3.1						
Overall completeness	98.7%						
Completeness in highest resolution shell	97.1%						
Overall R_{merge}	7.7%						
R_{merge} in highest resolution shell (2.38–2.30 Å)	39%						

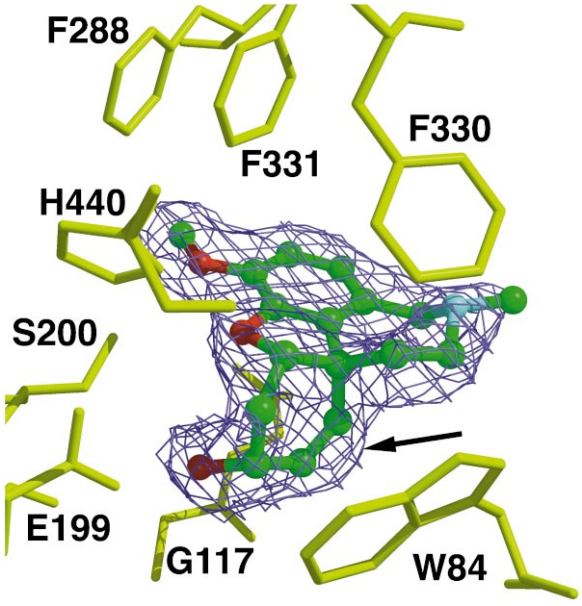

Fig. 2. Electron density map (Fo−Fc) from the GAL-*Tc*AChE complex after rigid body refinement. The map shows unambiguous density for GAL bound in the active site of the enzyme. Contouring level is at 3σ, shown in thin blue lines. Only contours within 2.0 Å of the inhibitor are shown. GAL is rendered as a ball-and-stick model, with carbon atoms colored green. Selected protein residues are rendered as sticks, with carbon atoms colored yellow and labeled appropriately. The double bond of the cyclohexene ring in GAL is indicated by the arrow (picture made with Xfit [42] and Raster3d [54]).

3. Results

The overall mode of binding of GAL to *Tc*AChE is shown in Fig. 3. The inhibitor binds at the base of the active site gorge, spanning the acyl-binding pocket and the choline-binding site, viz. the indole ring of Trp-84. There appear to be two classic hydrogen bonds formed with protein atoms (Fig. 4). One is between the hydroxyl group of the inhibitor and Glu-199 $O^{\varepsilon 1}$ (2.7 Å). The hydroxyl group also interacts with two water molecules. One water molecule (3.1 Å) is that which is bound in the oxyanion hole by the three NH groups of Gly-118, Gly-119 and Ala201. It is also bifurcated with the oxygen atom of the dihydrofuran ring of the inhibitor (3.1 Å). A second water molecule is 3.3 Å away and interacts also with Tyr-130 O^{η} and Gly-117 N. The second possible hydrogen bond to a protein atom involves the hydroxyl group of Ser-200, whose hydrogen may be bifurcated between His-440 $N^{\varepsilon 2}$

Table 2
Refinement results

Resolution range	30.0–2.3 Å
Number of protein atoms	4 211
Number of non-protein atoms	
Solvent (water, PEG)	144, 10
Carbohydrate atoms	28
Inhibitor	21
R_{work}	21.3%
R_{free} (5% of reflections)	25.0%
rms bond deviations	0.017 Å
rms angle deviations	1.8°

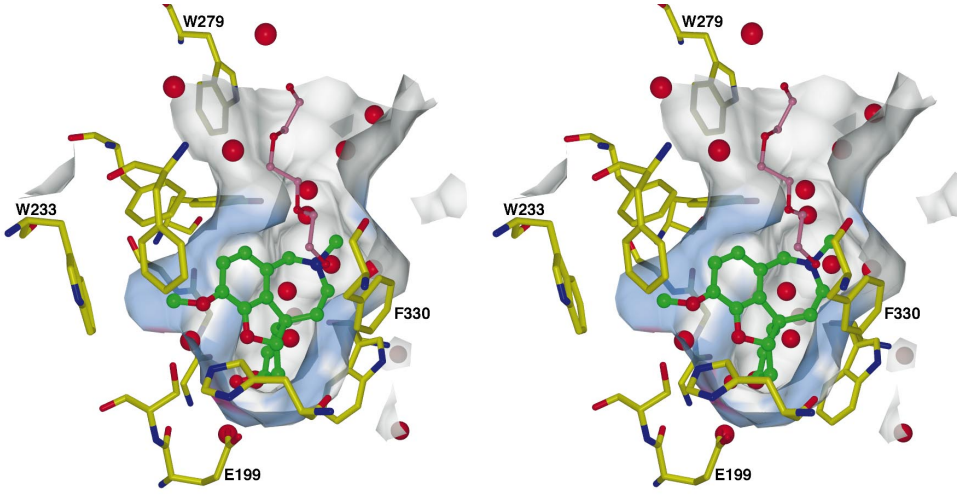

Fig. 3. Stereo view of binding of GAL in the active site gorge of *Tc*AChE. The solvent accessible surface of the protein (without waters and without ligands) was calculated by use of the program MSMS [55] with a probe radius of 1.4 Å. Only those parts of the surface within 9.0 Å of the bound inhibitor are visible, and the surface is 30% transparent, allowing visualization of some of the underlying protein residues. The surface has also been clipped to reveal the interior side, and has been color-coded such that blue indicates those parts of the surface whose underlying atoms are between 4.0 and 3.0 Å from any atom of the inhibitor, and pink indicates distances of less than 3.0 Å from the protein atoms to the inhibitor. Only a small portion of pink surface is visible in this orientation, located below the O-methyl group of the inhibitor, in the acyl-binding pocket. GAL has been rendered as a ball-and-stick model whose carbon atoms are colored green. Selected protein residues are shown as stick models with yellow carbon atoms. Water molecules are red spheres, and the PEG200 trimer/tetramer is rendered as a ball-and-stick model whose carbon atoms are colored pink (picture made with DINO [56] and rendered in POV-ray© [57]).

and the oxygen of the O-methyl group of the inhibitor. There may also be a non-classical hydrogen bond between the N-methyl group of the inhibitor and Asp-72 $O^{\delta 2}$ (3.4 Å), since the methyl group is expected to carry some of the positive charge of the amine. The unexpected presence of a PEG molecule in the active site gorge gives rise to an interesting interaction between the terminal hydroxyl group of the PEG molecule and the tertiary amine of GAL (2.8 Å). The terminal hydroxyl group, in turn, forms an aromatic hydrogen bond [45,46] with Phe-330. A water molecule could presumably fulfil the same role in the absence of PEG. The rest of the interactions between the inhibitor and the protein appear to be non-polar. This is particularly noteworthy, since the protonated tertiary amine group does not interact with Trp-84 or Phe-330 analogously to the interaction which is believed to occur between the quaternary amine of the natural substrate (acetylcholine) and the enzyme, and has been observed for a number of inhibitors [36,47,48]. In fact, the nitrogen and its three substituents are quite removed from Trp-84, the closest approach being between C11 of the inhibitor and C^{γ} (3.6 Å) and $C^{\delta 1}$ (3.7 Å) of the indole ring. The next methylene group in the tetrahydroazepine ring (C12) makes three contacts with the indole ring, and the rest of the interactions with Trp-84 involve the cyclohexene ring of GAL. The double bond in the cyclohexene ring stacks against the π system of the indole ring of Trp-84. Saturation of this double bond (to give lycoramine) greatly reduces the binding affinity of the inhibitor (T. Lewis, C. Personeni, unpublished results). On the opposite side of the gorge, the O-methoxy group of GAL occupies the acyl-binding pocket, contacting Phe-288 and Phe-290.

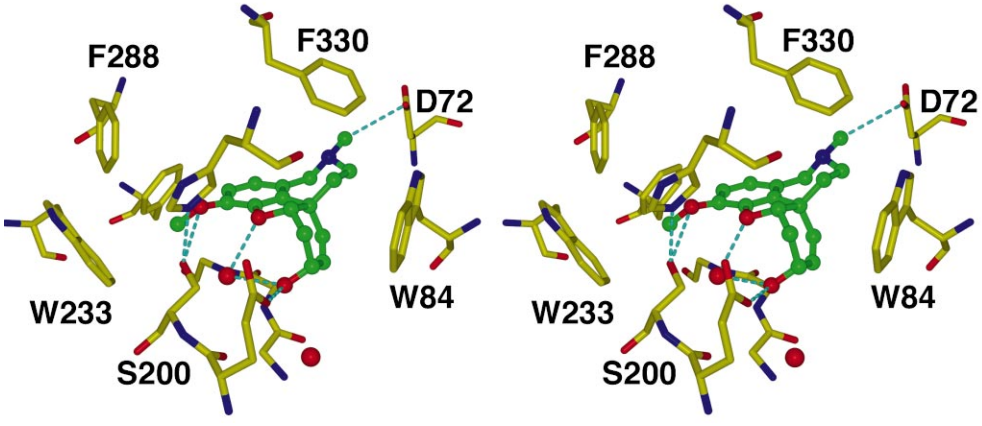

Fig. 4. Stereo view of possible hydrogen bonds between GAL and *Tc*AChE. The inhibitor is displayed as a ball-and-stick model, with green carbon atoms. The protein residues are rendered as stick models with yellow carbon atoms (DINO/POV-ray).

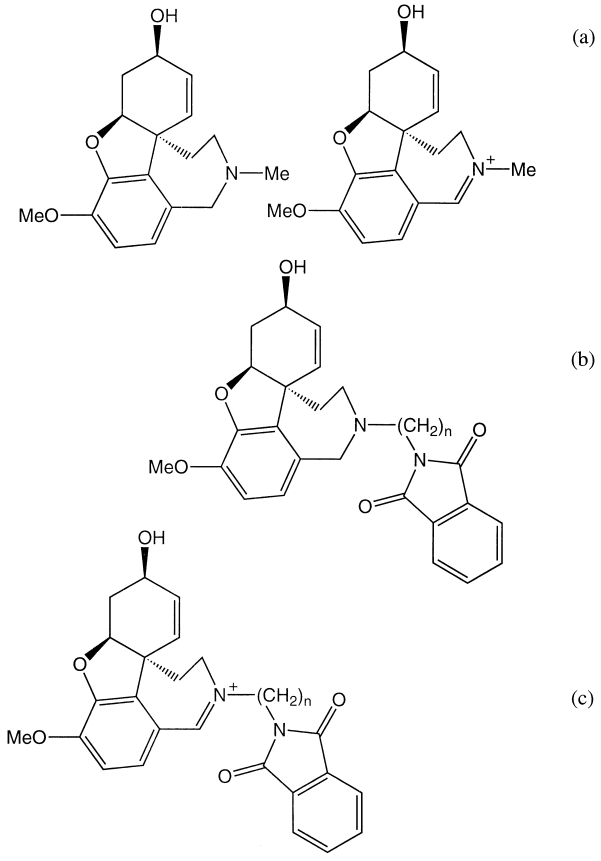

Fig. 5. (a) Comparison of GAL (left) with its iminium derivative (right). This is the same structure as in Fig. 1, but drawn here to show some of the stereochemistry. (b) GAL with N-linked phthalimide group using variable length alkyl chain. (c) Iminium derivative of GAL with N-linked phthalimide group, as in (b).

4. Discussion

Initial inspection of the GAL-*Tc*AChE complex does not reveal any specific interactions which could account for the tight binding observed. GAL is not a transition state analogue, which, of all the structures on the reaction coordinate, bind most tightly to the enzyme [49]. Nor are there any charge-charge interactions between the inhibitor and the enzyme. In fact, the only charged group in the inhibitor interacts rather indirectly with residues of the protein (through a solvent molecule to Phe-330, possibly via a methyl hydrogen to Asp-72, and via a methylene hydrogen with the π system of Trp-84). It must be assumed that the binding energy for GAL comes from a number of smaller enthalpic contributions, coupled to an unusually small entropic penalty. This latter point arises from the rigidity of the molecule, which allows the numerous interactions to occur with minimal loss of entropy. A similar concept is utilized in the tight binding of multisubstrate analogues ([50], see Fersht [51]).

Recent attempts to produce synthetic derivatives of GAL with higher binding affinities [38] showed that conversion of the tertiary amine to an iminium ion (See Fig. 5a) increased the affinity for electric eel AChE (*Ee*AChE) by 4.5-fold. In an attempt to produce bifunctional ligands which would interact with Trp-279 at the top of the gorge, a phthalimido group was attached to the nitrogen (Fig. 5b), via alkyl spacers of varying lengths. This had only a moderate effect on the IC_{50}, with a maximal decrease of 5.6-fold (four-carbon spacer), and a maximal increase of only 1.3-fold (eight-carbon spacer), relative to GAL. Interestingly, a molecule combining both the iminium and pthalimido (eight-carbon spacer) modifications (Fig. 5c) showed a 36-fold increase in affinity. The crystal structure of GAL bound in the active site of *Tc*AChE justifies the above rationale for creating bis-interacting derivatives, since the nitrogen atom is oriented up the gorge. This is in contrast to the results obtained when attachment of the alkyl-phthalimido functionality was via the hydroxyl group of GAL. The compounds so obtained inhibit AChE approximately two orders of magnitude more weakly than GAL itself. Since the observed binding mode of GAL places the hydroxyl group in an area of restricted volume, additions to this part of the molecule would presumably force GAL to bind in a different fashion. What is not apparent is why the iminium derivative should be a better inhibitor than native GAL, since the latter is presumably protonated at pH 5.6. One possibility is that the

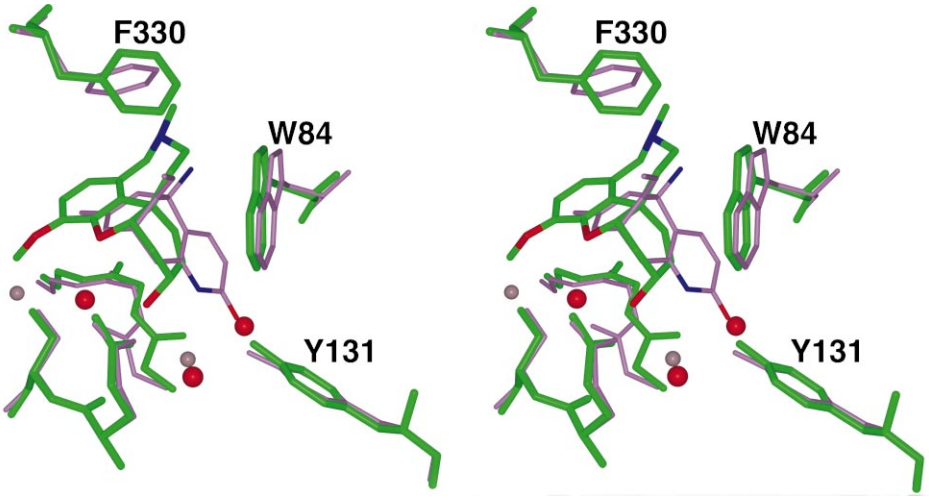

Fig. 6. Stereo view comparing binding of GAL and huperzine A in the active site of *Tc*AChE, showing the main chain conformational change (Gly-117) associated with binding of huperzine A. GAL and associated protein residues are rendered as green stick models, while huperzine and associated protein residues are rendered as thin pink stick models. Water molecules associated with the GAL structure are shown as red spheres, while those from the huperzine structure are displayed as smaller pink spheres (DINO/POV-ray).

planar geometry of the nitrogen atom allows closer interaction of the N-methyl group with Asp-72, resulting in a stronger hydrogen bond.

Another AD drug, huperzine A [36,52], shares common binding characteristics with GAL (Fig. 6). Both molecules have a bent hinge shape and, in both cases, the hinge is oriented similarly when the ligand is bound to *Tc*AChE. Both molecules pack against the face of Trp-84 and make few direct hydrogen bonds to the protein. Nevertheless, there are several major differences in their binding modes. Thus, GAL does not induce a main chain conformational change at Gly-117 as does huperzine A. Moreover, the orientation of the side chain of Phe-330 differs in the two complexes. Furthermore, the primary amino group of huperzine A interacts much more closely with the indole ring of Trp-84 than does the tertiary amine of GAL. Finally, GAL does not exhibit the slow binding kinetics observed for huperzine A [53]. A partial answer to the question of why GAL binds with a tightness comparable to huperzine A, despite apparent lack of direct interaction between the amine group and Trp-84, may lie in the fact that GAL fills more of the active site volume, since it also binds in the acyl-binding pocket. Furthermore, one of the direct hydrogen bonds with the protein involves a charged residue (Glu-199), which is not the case for huperzine A.

5. Conclusions

The structure of the complex of GAL and *Tc*AChE shows that GAL binds at the base of the gorge interacting with both the acyl-binding pocket and the principal quaternary ammonium-binding site, the indole ring of Trp-84. The high affinity displayed by the inhibitor for AChE appears to come from a number of moderate to weak interactions accompanied by a low entropic cost owing to its rigid structure.

Acknowledgements: This work was supported by the U.S. Army Medical and Materiel Command under Contract No. DAMD17-97-2-7022, the EU 4th Framework Program in Biotechnology, the Kimmelman Center for Biomolecular Structure and Assembly (Rehovot, Israel), and the Dana Foundation. The generous support of Mrs. Tania Friedman is gratefully acknowledged. I.S. is a Bernstein-Mason Professor of Neurochemistry.

References

[1] Bartus, R.T., Dean, R.L., Beer, B. and Lippa, A.S. (1982) Science 217, 408–414.
[2] Dunnett, S.B. and Fibiger, H.C. (1993) Prog. Brain Res. 98, 413–420.
[3] Weinstock, M. (1997) J. Neural Transm. 49, 93–102.
[4] Wu, E.S., Griffith, R.C., Loch, J.T., Kover, A., Murray, R.J., Mullen, G.B., Blosser, J.C., Machulskis, A.C. and McCreedy, S.A. (1995) J. Med. Chem. 38, 1558–1570.
[5] Brandeis, R., Dachir, S., Sapir, M., Levy, A. and Fisher, A. (1990) Pharmacol. Biochem. Behav. 36, 89–95.
[6] Enz, A., Amstutz, R., Boddeke, H., Gmelin, G. and Malanowski, J. (1993) Prog. Brain Res. 98, 431–438.
[7] Weinstock, M. (1995) Neurodegeneration 4, 349–356.
[8] Jenike, M.A., Albert, M.S., Heller, H., Gunther, J. and Goff, D. (1990) J. Clin. Psychiatr. 51, 3–7.
[9] Zhang, R.W., Tang, X.C., Han, Y.Y., Sang, G.W., Zhang, Y.D., Ma, Y.X., Zhang, C.L. and Yang, R.M. (1991) Acta Pharmacol. Sin. 12, 250–252.
[10] Davis, K.L. and Powchik, P. (1995) Lancet 345, 625–630.
[11] Weinstock, M., Razin, M., Chorev, M. and Enz, A. (1994) J. Neural Transm. 43, 219–225.
[12] Knopman, D.S. (1998) Neurology 50, 1203–1206.
[13] Kawakami, Y., Inoue, A., Kawai, T., Wakita, M., Sugimoto, H. and Hopfinger, A.J. (1996) Bioorg. Med. Chem. 4, 1429–1446.
[14] Kryger, G., Silman, I. and Sussman, J.L. (1999) Structure 7, 297–307.
[15] As reported on the Sanochemia web site, under the information concerning galanthamine, http://www.sanochemia.at/.
[16] Bretagne, M. and Valletta, J. (1965) Anesth. Analg. (Paris) 22, 285–292.
[17] Harvey, A.L. (1995) Pharmacol. Ther. 68, 113–128.
[18] Bystrzanowska, T. (1969) Wiad Lek 22, 1233–1239.
[19] Gujral, V.V. (1965) Indian Pediatr. 2, 89–93.
[20] Thomsen, T. and Kewitz, H. (1990) Life Sci. 46, 1553–1558.
[21] Thomsen, T., Kaden, B., Fischer, J.P., Bickel, U., Barz, H., Gusztony, G., Cervos-Navarro, J. and Kewitz, H. (1991) Eur. J. Clin. Chem. Clin. Biochem. 29, 487–492.
[22] Schrattenholz, A., Pereira, E.F., Roth, U., Weber, K.H., Albuquerque, E.X. and Maelicke, A. (1996) Mol. Pharmacol. 49, 1–6.
[23] Storch, A., Schrattenholz, A., Cooper, J.C., Abdel Ghani, E.M., Gutbrod, O., Weber, K.H., Reinhardt, S., Lobron, C., Hermsen, B., Soskiç, V., Pereira, E.F.R., Albuquerque, E.X., Methfessel, C. and Maelicke, A. (1995) Eur. J. Pharmacol. 290, 207–219.
[24] Pereira, E.F., Reinhardt-Maelicke, S., Schrattenholz, A., Maelicke, A. and Albuquerque, E.X. (1993) J. Pharmacol. Exp. Ther. 265, 1474–1491.
[25] Prendergast, M.A., Jackson, W.J., Terry Jr., A.V., Decker, M.W., Arneric, S.P. and Buccafusco, J.J. (1998) Psychopharmacology (Berl.) 136, 50–58.
[26] Arendash, G.W., Sengstock, G.J., Sanberg, P.R. and Kem, W.R. (1995) Brain Res. 674, 252–259.
[27] De Sarno, P. and Giacobini, E. (1989) J. Neurosci. Res. 22, 194–200.
[28] Kem, W.R. (1997) Invert. Neurosci. 3, 251–259.
[29] Lloyd, G.K., Menzaghi, F., Bontempi, B., Suto, C., Siegel, R., Akong, M., Stauderman, K., Velicelebi, G., Johnson, E., Harpold, M.M., Rao, T.S., Sacaan, A.I., Chavez-Noriega, L.E., Washburn, M.S., Vernier, J.M., Cosford, N.D. and McDonald, L.A. (1998) Life Sci. 62, 1601–1606.
[30] Newhouse, P.A., Potter, A. and Levin, E.D. (1997) Drugs Aging 11, 206–228.
[31] Wevers, A., Monteggia, L., Nowacki, S., Bloch, W., Schutz, U., Lindstrom, J., Pereira, E.F., Eisenberg, H., Giacobini, E., De Vos, R.A., Steur, E.N., Maelicke, A., Albuquerque, E.X. and Schroder, H. (1999) Eur. J. Neurosci. 11, 2551–2565.
[32] Stein, K. (1996) Inpharma 4, 1019.
[33] Berger, A. (1999) BMJ 318, 639.
[34] Kubinyi, H. (1999) J. Recept. Signal Transduct. Res. 19, 15–39.
[35] Amzel, L.M. (1998) Curr. Opin. Biotechnol. 9, 366–369.
[36] Raves, M.L., Harel, M., Pang, Y.P., Silman, I., Kozikowski, A.P. and Sussman, J.L. (1997) Nat. Struct. Biol. 4, 57–63.
[37] Harel, M., Kleywegt, G.J., Ravelli, R.B., Silman, I. and Sussman, J.L. (1995) Structure 3, 1355–1366.
[38] Mary, A., Renko, D.Z., Guillou, C. and Thal, C. (1998) Bioorg. Med. Chem. 6, 1835–1850.
[39] Otwinowski, Z. (1993) in: Data Collection and Processing (Sawyer, L., Isaacs, N. and Bailey, S., Eds.), Proceedings of the CCP4 Study Weekend 29–30 January 1993, pp. 56–62, SERC, Daresbury.
[40] Collaborative Computational Project, Number 4 (1994) Acta Crystallogr. Sect. D Biol. Crystallogr. 50, pp. 760–763.
[41] Brunger, A.T., Adams, P.D., Clore, G.M., DeLano, W.L., Gros, P., Grosse-Kunstleve, R.W., Jiang, J.S., Kuszewski, J., Nilges, M., Pannu, N.S., Read, R.J., Rice, L.M., Simonson, T. and Warren, G.L. (1998) Acta Crystallogr. D. Biol. Crystallogr. 54, 905–921.
[42] McRee, D.E. (1999) J. Struct. Biol. 125, 156–165.
[43] Carroll, P., Furst, G.T., Han, S.Y. and Joullié, M. (1990) Bull. Soc. Chim. Fr. 127, 769–780.
[44] Brunger, A.T., Adams, P.D. and Rice, L.M. (1999) Prog. Biophys. Mol. Biol. 72, 135–155.
[45] Burley, S.K. and Petsko, G.A. (1986) FEBS Lett. 203, 139–143.
[46] Levitt, M. and Perutz, M.F. (1988) J. Mol. Biol. 201, 751–754.
[47] Harel, M., Schalk, I., Ehret Sabatier, L., Bouet, F., Goeldner,

M., Hirth, C., Axelsen, P.H., Silman, I. and Sussman, J.L. (1993) Proc. Natl. Acad. Sci. USA 90, 9031–9035.
[48] Harel, M., Quinn, D., Nair, H., Silman, I. and Sussman, J. (1996) J. Am. Chem. Soc. 118, 2340–2346.
[49] Lienhard, G.E. (1973) Science 180, 149–154.
[50] Collins, K.D. and Stark, G.R. (1971) J. Biol. Chem. 246, 6599–6605.
[51] Fersht, A.R. (1977) Enzyme Structure and Mechanism, W.H. Freeman, Reading.
[52] Liu, J.-S., Zhu, Y.-L., Yu, C.-M., Zhou, Y.-Z., Han, Y.-Y., Wu, F.-W. and Qi, B.-F. (1986) Can. J. Chem. 64, 837–839.
[53] Ashani, Y., Peggins, J.O. and Doctor, B.P. (1992) Biochem. Biophys. Res. Commun. 184, 719–726.
[54] Merritt, E.A. and Bacon, D.J. (1997) Methods Enzymol. 277, 505–524.
[55] Sanner, M.F., Olson, A.J. and Spehner, J.C. (1996) Biopolymers 38, 305–320.
[56] Phillippsen, A. (1999) DINO: Visualizing Structural Biology, http://www.bioz.unibas.ch/–xray/dino.
[57] POV-ray-Team™ (1998) POV-ray, www.povray.org.